

Interaction of a smoothed laser beam with supercritical-density porous targets on the ABC facility

C. Strangio, A. Caruso, S.Yu. Gus'kov, V.B. Rozanov, A.A. Rupasov

Abstract. We present the results of experiments on the interaction of laser radiation with low-density porous targets performed on the ABC facility at the ENEA Research Centre (Frascati, Italy). Porous plastic targets with densities of 5 and 20 mg cm⁻³ were irradiated by a focused neodymium-laser beam at the fundamental frequency ($\lambda = 1.054 \mu\text{m}$) at a radiation intensity of $10^{13} \text{ W cm}^{-2}$ at the target. The beam was preliminarily allowed to pass through an optical system intended to spatially smooth the radiation intensity over the beam cross section. The use a smoothed beam was important to discover in the plasma and in the accelerated dense material the features related to the porous structure of the target under conditions which rule out the effect of the inhomogeneities of the heating beam itself. The spatial plasma structure in the laser beam–target interaction region and at the rear side of the target were investigated by using optical schlieren plasma photography. The time dependent transmission of the laser radiation through the target was also investigated by imaging the target in transmitted radiation to a properly masked photodiode.

Keywords: interaction of laser radiation with a plasma, porous material, transmission of laser radiation through a target.

1. Introduction

Experiments performed earlier on the ABC facility [1, 2] have shown that there occurs efficient (above 80%) absorption of the energy of 1.054- μm nanosecond laser pulses interacting with a low-density material with the supercritical density, i.e., with a material with the average density ρ_a exceeding the critical density ρ_{cr} for the given wavelength [$\rho_a > \rho_{cr} = 3.1 \text{ mg cm}^{-3}$ for fully ionised polystyrene (CH)_n]. These data were interpreted by assuming that a cavity was formed inside the target material, where the laser radiation was trapped [1]. Such an interaction scenario was confirmed by numerical calculations per-

formed for homogeneous systems with a density equal to ρ_a . These calculations were performed employing the CoBi3 code, which involved a real description of the experiment within the framework of the ray-optics approximation [1].

Laser radiation in experiments [1, 2] was focused by an aspheric lens with the numerical aperture $F/0.8$ to produce the power density of $2 \times 10^{14} \text{ W cm}^{-2}$ at the target surface. The experiments demonstrated a hydrodynamic flow pattern that was consistent with the results of numerical simulations. It was found that the motion of a dense material eventually resulted in an analogue of spherical expansion which was accompanied by the formation of thin substructures (jets) supposedly due to the porous material structure and to the spatially inhomogeneous structure of the incident beam. These initial inhomogeneities lead to the development of hydrodynamic instabilities upon acceleration of a dense material by a low-density material according to the ‘snow plough’ model [1].

The new experiments, like those carried out earlier, were performed by using a neodymium-glass laser (the ABC facility) with a quasi-triangular radiation pulse with the full width at half-maximum (FWHM) of 3 ns and a spectral width of 0.15 THz at $\lambda = 1.054 \mu\text{m}$. The focusing system used in these experiments involved a 2-D matrix of 256 lenses with a randomly distributed thickness to smooth out the spatial beam structure [the so-called induced smoothing incoherence (ISI) technique]. The smoothed laser beam [3] was focused on the target surface to produce a power density of $10^{13} \text{ W cm}^{-2}$.

The beam structure smoothing technique is described in Ref. [3]. As an illustration, Fig. 1 shows the measured laser intensity distribution in the focal plane of the focusing lens (where the target surface under irradiation is usually located). The distribution is characterised by the existence of a plateau of size 400 by 400 μm . The beam dimension and the intensity distribution over its cross section are retained over a length of 400 μm along the optical axis ($\pm 200 \mu\text{m}$ on either side of the focal plane) [3]. This means that the irradiation conditions are not changed substantially due to the motion of the absorbing region. The spatial Fourier analysis of the focal spot shows that the relative amplitudes of the modes with numbers $n \geq 6$ is less than 1% and is about 0.1% for the modes with $n \geq 10$. The use of a smoothed beam to irradiate porous targets permits revealing the special features of the spatial structure of the plasmas at the front and rear sides of the target, which are determined by the structure of the porous material itself.

The initial radiation penetration into the target may be different for different regions of the beam cross section,

C. Strangio, A. Caruso Associazione EUROATOM-ENEA sulla Fusione, C.R.E. Frascati, Via E. Fermi, C.P. 65, 00044, Frascati, Roma, Italia;

S.Yu. Gus'kov, V.B. Rozanov, A.A. Rupasov P.N. Lebedev Physics Institute, Russian Academy of Sciences, Leninsky prosp. 53, 119991 Moscow, Russia; e-mail: guskov@sci.lebedev.ru

Received 17 June 2005; revision received 9 March 2006

Kvantovaya Elektronika 36(5) 424–428 (2006)

Translated by E.N. Ragozin

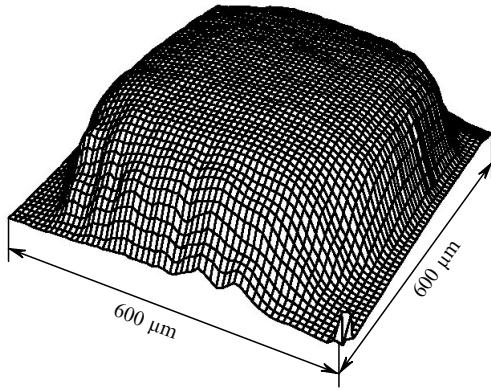


Figure 1. Spatial intensity distribution of the target-irradiating laser beam. A uniform intensity plateau of size 400 by 400 μm is observed.

depending on the structure of the porous material (cells with a different wall thickness, communicating cells). When the cell walls explode, the material density distribution equalises on the cellular scale due to the propagation and collisions of shock waves and to the viscosity mechanism [1, 2]. The latter should eliminate the local density fluctuations remaining after the internal collapse of the pores and the interaction of shock waves.

In our experiments, we used porous plastic targets with densities of 5 and 20 mg cm^{-3} , their respective cell dimensions being equal to ~ 70 and ~ 40 μm for a wall thickness of about 1 μm . The calculations performed in [1, 2] for structures with such parameters show that for these density fluctuations the relaxation time due to viscosity (several nanoseconds) is much longer than the pore collapse time (fraction of a nanosecond) and turns out to be longer than the laser-pulse duration for the radiation intensities employed in the experiment. This means that the plasma density inhomogeneities may persist over the entire interaction period. In this case, the plasma may be locally subcritical, despite the fact that its volume-averaged density is supercritical. This permits the radiation to penetrate through subcritical-density plasma regions, whose position varies with time.

In principle, some light penetration through the target may occur during the interaction period (with oscillations of the transmission coefficient). Such a behaviour is most likely when $\rho_a > \rho_{cr}$ and $(\rho_a - \rho_{cr})/\rho_a \ll 1$, which is certainly fulfilled for targets with a density of 5 mg cm^{-3} . This process is related to a possible difference in initial light transmission of different regions of the laser spot and may result in the initial production of a numerous absorbing cavities.

The targets used in these experiments had normally the shape of a parallelepiped with transverse dimensions exceeding the focal spot size, which ruled out the passage of laser radiation past the targets. The product of the average target density ρ by their thickness s was varied in the range between 3000 and 8000 $\mu\text{m mg cm}^{-3}$. We studied the hydrodynamics of laser radiation–target interaction by means of optical schlieren photography and of light transmission through the targets for the values of ρs lying in the above-mentioned range.

2. Hydrodynamic features of radiation–target interaction

We investigated the hydrodynamic evolution of a target by the optical schlieren photography technique. The target was probed by the second harmonic (2ω) laser beam in the direction orthogonal to the axis of the heating beam; the probe pulse duration was 0.5 ns [1].

Typical results are shown in Fig. 2, where the photographs are presented in the order of increasing the ρs value and correspond to instant $t = 3$ ns from the onset of the heating radiation pulse. The thinnest target (shot No. 310) is accelerated, and the relatively dense material moving on its rear side appears like a curved dark region behind a thin white contour, which indicates the initial configuration of the unperturbed target. Within the framework of the ‘snow plough’ model, the velocity of material motion can be calculated from the position of the boundary of this dark region and is equal to 10^7 cm s^{-1} . The existence of the boundary of the opaque region indicates that there are no large-scale ruptures (Fig. 3). This may mean that the stage of pores collapse with the formation of numerous

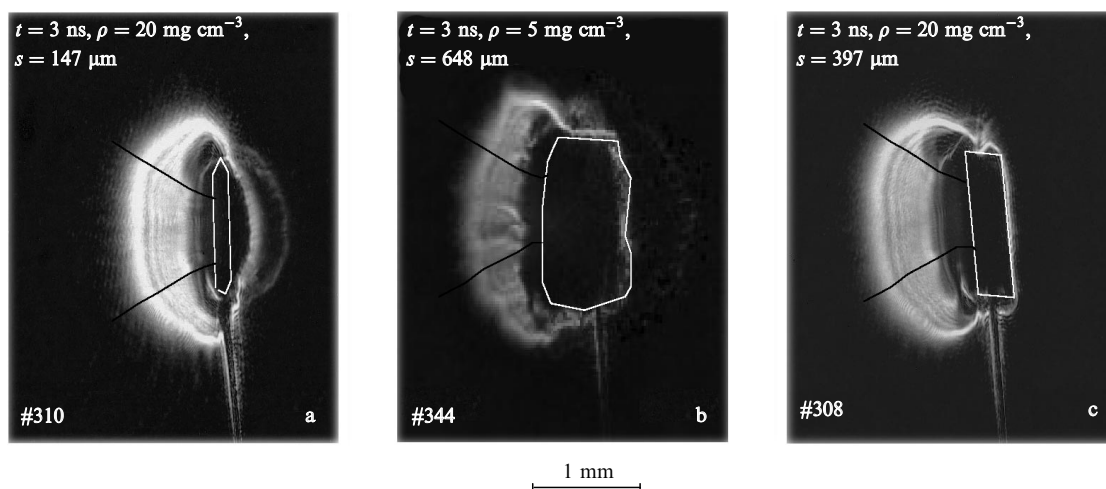


Figure 2. Schlieren photographs of porous polystyrene targets irradiated by a smoothed laser beam for $\rho s = 2940$ (a), 3240 (b), and 7940 $\mu\text{m mg cm}^{-3}$ (c). White contours indicate the initial target configurations and the black lines show the boundaries of the focused laser beam.

cavities with a lower density, discussed in the previous Section, is completed by the instant $t = 3$ ns, and the density distribution corresponds to the uniform plasma state. At the same time, however, thin jet-like structures are observed at the boundary of the accelerated dense material on the rear side of the target. For thicker targets (shots No. 344 and 308), at the instant $t = 3$ ns, the 'snow plough' structure is still inside the target, and therefore the acceleration of the dense material on the rear side of the target is not observed.

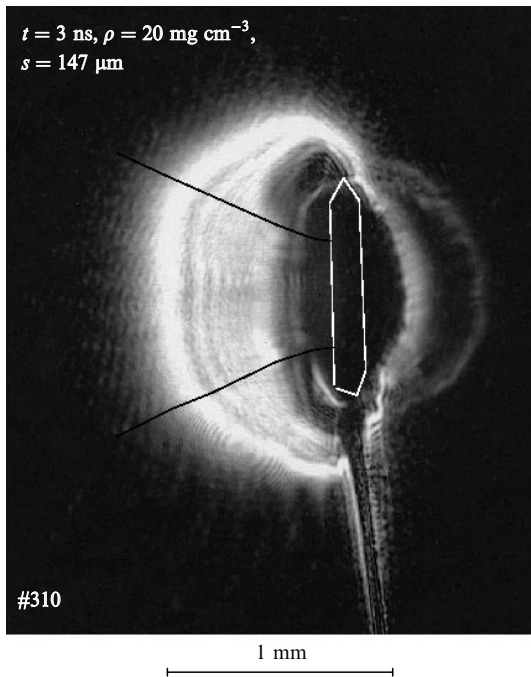


Figure 3. Magnified schlieren photograph for shot No. 310. A thin jet-like structure is clearly seen at the rear side of the dense accelerated material.

As for the structure of the plasma produced on the front side of the target, for a material with small cells (20 mg cm^{-3} , shots No. 310 and 308) it is relatively uni-

form, whereas for a target with large cells (5 mg cm^{-3} , shot No. 344), the plasma corona with a substantially stronger turbulence is observed. At the rear side of the targets with a small ρs product (shots No. 310 and 344), a plasma structure is observed, which is absent for the target with a large ρs (shot No. 308) at the instant $t = 3$ ns.

3. Investigation of laser radiation passage through the target

We investigated the propagation of a laser pulse through the target by using the setup shown in Fig. 4. The temporal shape of the laser pulse was recorded with a photodiode $\text{PD}\omega$. The laser radiation transmitted through the target was converted to the second harmonic in a KDP crystal, and the target image in this radiation was focused to a photographic camera and a $\text{PD}2\omega$ photodiode using lenses 2 and 3. This nonlinear conversion was necessary to match the selective spectral sensitivity of the photodiode. A special mask was placed on the target image on the $\text{PD}2\omega$ photodiode. This was done to separate the target region that transmits the radiation (this region is normally smaller than the focal spot, see Fig. 5). The time-dependent target transmission coefficient was measured in working shots according to the algorithm described below. The measurement data were normalised on the basis of auxiliary shots in the absence of targets (all other conditions being the same) taking into account the dependence of the second harmonic conversion efficiency on the radiation intensity incident on the crystal.

For the optical experiment setup (taking into account the quadratic dependence of the nonlinear radiation conversion coefficient in the crystal), the voltage $V_{2\omega}(t)$ measured by the $\text{PD}2\omega$ photodiode is a function of the voltage $V_{\omega}(t)$ measured by the $\text{PD}\omega$ photodiode:

$$V_{2\omega}(t) = f\delta(t)t_r^2(t)V_{\omega}^2(t), \quad (1)$$

where f is the transmission coefficient of the filter placed in front of the $\text{PD}2\omega$ photodiode; $t_r(t)$ is the target transmission coefficient; and the function $\delta(t)$ is determined from

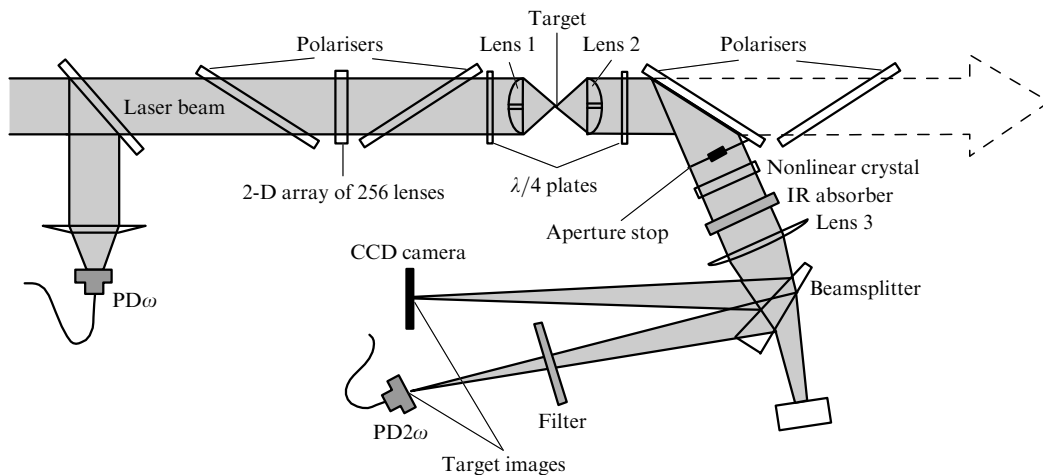


Figure 4. Setup for measuring the intensity of laser radiation transmitted through the target and for forming the target image with the transmitted laser beam.

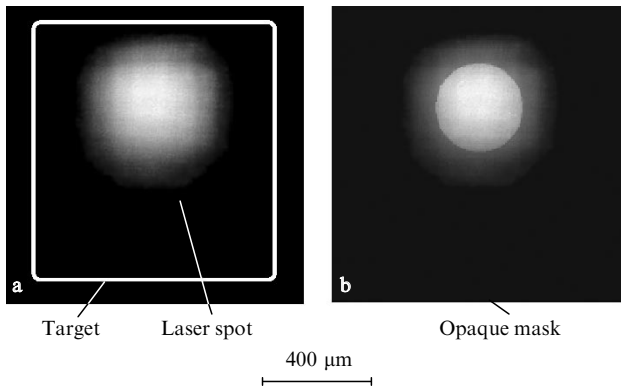


Figure 5. Mutual arrangement and dimensions of the target and of the laser focal spot on the target image formed on the PD 2ω photodiode (the laser spot image was obtained in the absence of the target and then combined with its typical cross section) (a) and diaphragming of the laser spot with a circular mask (the mask material is opaque; however, to show the relative dimensions of the circular aperture of the mask and the laser spot, it is shown as being partly transparent) (b).

the measurements in the shots made in the absence of the target [$t_r(t) = 1$] from the expression

$$\delta(t) = \frac{V_{02\omega}(t)}{f_0 V_{0\omega}^2(t)}; \quad (2)$$

the subscript 0 means the absence of the target. Then, the time-dependent target transmission coefficient $t_r(t)$ is determined from the expression

$$t_r(t) = \frac{V_{2\omega}(t)}{[f\delta(t)V_{\omega}^2(t)]^{1/2}}. \quad (3)$$

Because the bandwidth of the system employed to record the electric signal was equal to 5 GHz, the method enabled us to perform measurements with a time resolution equal to a fraction of the laser pulse duration. The measurement data are presented in Fig. 6. The most reliable part of the data is related to the first three nanoseconds. For $t > 3$ ns, the amplitudes of the signals are low, so that relation (3) becomes essentially ambiguous. We found that the target transmission coefficient for these shots varied between 0.005 and 0.010 during the first three nanoseconds. The time dependences of the target transmission coefficients integrated over the interaction region are modulated in time with a characteristic period of 0.3–0.5 ns. These modulations may be caused by the formation of local subcritical-density cavities discussed above. Note that local time variations of the transmission coefficient are preserved in the space-integrated signal.

We studied the properties of laser radiation transmitted through the plasma of porous targets. These experiments were performed for a substantially sharper focusing of the laser beam. In particular, the temporal and angular characteristics of transmitted laser radiation at the second harmonic frequency (0.53 μm) of a neodymium laser were measured at the P.N. Lebedev Physics Institute [4, 5] for a sharp beam focusing on the surface of a polypropylene porous target with a density of 20 mg cm^{-3} and a thickness of 200–800 μm . For $\lambda = 0.53$ μm , the critical material density is equal to 12.5 mg cm^{-3} , and, therefore, the targets possessed the supercritical average

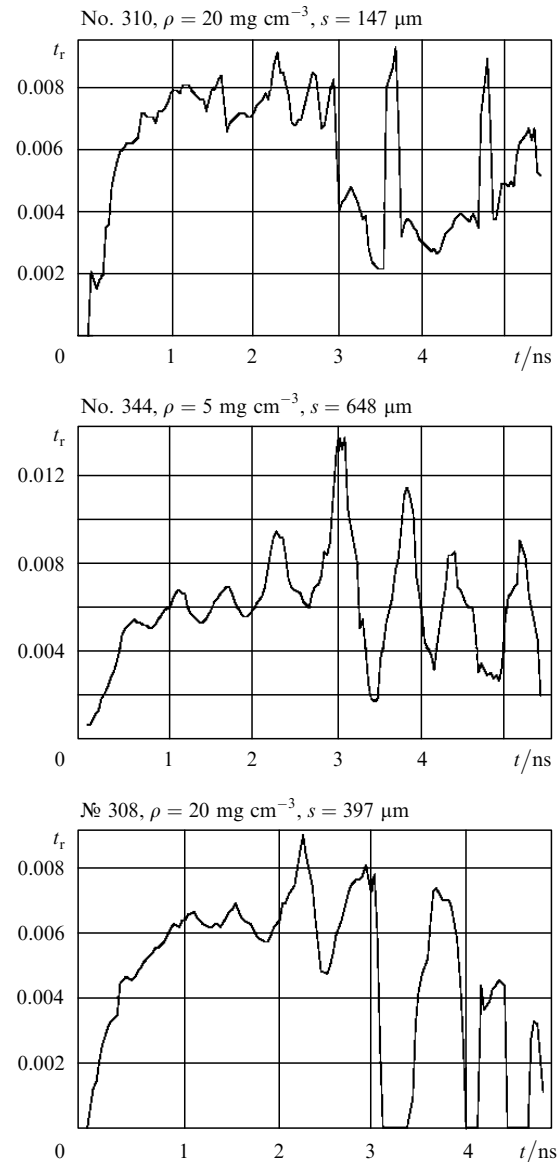


Figure 6. Time dependences of the target transmission coefficient for selected shots.

density. The focal spot diameter was 15 μm and the radiation intensity was 5×10^{14} W cm^{-2} . The time modulations of transmitted radiation with a typical time scale of less than 100 ps were observed [4, 5], which were accompanied by a sharp increase in the scattering angles for the transmitted radiation (up to 15°). This increase was observed at the moment the target was burned through, i.e. at the moment the high-intensity laser signal (in the paraxial part of the beam) reached the rear side of the target. Such a temporal modulation was interpreted as the manifestation of self-focusing in a plasma. The time required to burn the target through depended on its thickness and was equal, for instance, to 1 and 2 ns for 200- and 400- μm thick targets, respectively.

The fraction of laser radiation transmitted through a planar layer of porous material was measured at the TRINITI (the Troitsk Institute for Innovation and Fusion Research) [6] upon irradiating agar targets by the 3-ns, 10^{14} - W cm^{-2} fundamental radiation pulses of a neodymium laser. The targets had different thickness, which was varied

between 100 and 1000 μm . The average agar–agar densities were also different and ranged between 0.5 and 10 mg cm^{-3} . Because the critical density of this material for the above laser wavelength is close to 3 mg cm^{-3} , the targets were sub- or near-critical in density. The time-integrated measurements for targets with a thickness exceeding 500 μm showed that the fraction of laser radiation transmitted through the target did not exceed 0.001. In going over to thinner targets (200–300 μm) with a low density (0.5–1 mg cm^{-3}), the fraction of transmitted radiation was observed to increase sharply up to 0.02. Time-resolved measurements showed that the radiation pulse transmitted through the target was recorded at the end of the laser pulse action. The transmitted-pulse duration was 300–500 ps. The increase in the target transmittance was explained in [6] by the completion of plasma homogenisation, which resulted in the formation of a subcritical-density plasma.

Therefore, the data obtained in different experiments on laser radiation transmission suggest that the spatiotemporal characteristics of the state of porous target plasmas, including their optical properties, are substantially dependent on target irradiation conditions as well as on the structure, density, and thickness of the targets.

4. Conclusions

Experiments on the laser irradiation of porous targets showed that the exposure of foils (thin targets) to a smoothed laser beam results in material acceleration without ruptures at the interface between the plasma and the rear side of the target.

The plasma structure at the front side of a higher-density (small-cell) target is relatively uniform, whereas a turbulent plasma corona is produced in the case of a lower-density (large-cell) target. On the rear side of the targets with a small ρs product a plasma structure is detected, which is absent for targets with large ρs till the completion of the laser pulse.

We have measured the time dependence of the target transmission for laser radiation. The typical target transmission coefficients ranged from 0.005 to 0.010.

Acknowledgements. The authors thank P.L. Andreoli and G. Cristofari for their technical assistance in the experiments, and the engineer A. Dattola for providing the energy supply to the facility and the operation of vacuum and air conditioning systems. This work was supported by the Russian Foundation for Basic Research (Grant Nos 04-02-17671, 05-02-17873, and 05-02-16856).

References

1. Caruso A., Strangio C., Gus'kov S.Yu., Rozanov V.B. *Laser Part. Beams*, **18**, 25 (2000).
2. Gus'kov S.Yu., Caruso A., Rozanov V.B., Strangio C. *Kvantovaya Elektron.*, **30** (3), 191 (2000) [*Quantum Electron.*, **30** (3), 191 (2000)].
3. Strangio C., Caruso A. *Laser Part. Beam.*, **16**, 45 (1998).
4. Gus'kov S.Yu., Kas'yanov Yu.S., Koshevoi M.O., Rozanov V.B., Rupasov A.A., Shikanov A.S. *Pis'ma Zh. Eksp. Teor. Fiz.*, **64** (7), 462 (1996).
5. Gus'kov S.Yu., Kas'yanov Yu.S., Koshevoi M.O., Rozanov V.B., Rupasov A.A., Shikanov A.S. *Laser Part. Beam.*, **17** (2), 287 (1999).
6. Bugrov A.E., Burdonskii I.N., Gavrilov V.V., et al. *Zh. Eksp. Teor. Fiz.*, **115** (3), 803 (1999).